Opto-electronics **4** *(1972) 69–86*

REVIEW

Tunable infra-red lasers and their applications to air pollution measurements*

E. D. HINKLEY
MIT Lincoln Laboratory, Lexington, Massachusetts, USA

Received 5 May 1972

This paper describes a number of tunable infra-red lasers and techniques employing them for the detection and monitoring of gaseous air pollutants. Recent progress in the development of lasers that can be matched to characteristic infra-red absorption or emission lines of certain pollutants suggest wide potential application for sensitive specific monitoring. Examples to be described include highly-specific point-sampling, *in situ* source monitoring, ambient air monitoring, resonance fluorescence, and remote heterodyne detection.

1. Introduction

The use of fixed-frequency gas lasers for air pollution detection has been suggested and advanced by several workers over the last few years [1]. By selecting appropriate laser transitions which overlap those of the gaseous pollutants, their concentrations can be measured by direct absorption. However, the match is seldom ideal; and for some important pollutant gases, such as SO_2, there appear to be no entirely satisfactory laser lines. Even when overlaps are found, there may be other reasons why a selected gas laser line is not suitable; such as absorption by other components of the normal atmosphere, or coincidence (interference) with spectral lines of other pollutants which may be present.

During the past two years substantial progress has been made in the development of several types of tunable lasers, and systems utilizing these devices are being built for point-sampling and *in situ* source monitoring. Tunable infra-red lasers have also been proposed for ambient air monitoring [2] (both at ground level and in the upper atmosphere) and for single-ended, remote heterodyne detection of emissions from stationary or mobile sources [3].

A brief survey will be given of the various types of tunable lasers, followed by a discussion of monitoring techniques which can be used. Most of the experimental results represent work performed in our laboratory using current-tuned semiconductor diode lasers, although work performed by others will also be described, for completeness. Two recently-published articles can provide general background information for laser

*This work was supported by the Environmental Protection Agency.

© *1972 Chapman and Hall Ltd.*

techniques. Kildal and Byer [4] compare in detail laser Raman scattering, resonance fluorescence, and tunable laser absorption techniques. Melngailis [5] covers in more detail the direct absorption techniques and tunable semiconductor lasers.

2. Tunable lasers

Table I lists the types of tunable lasers which are presently available or under development. We consider only primary tunable laser sources, although other wavelengths are possible by mixing radiation from a tunable laser with that from a fixed-frequency laser [6].

TABLE I Tunable lasers

	Approximate coverage (μm)	Single-mode CW output (W)	Pulsed output (W)
Organic dye lasers	0.34– 1.2	5×10^{-2}	10^7
Parametric oscillators	0.5 – 3.75	3×10^{-3}	10^5
Semiconductor diode lasers	0.63–34	10^{-3}	10^2
Spin-flip Raman lasers	5.3 – 6.2 (CO) 9.2 –14 (CO_2)	1	10^3
Bulk semiconductor lasers (optically-pumped)	0.32–34*	10^{-3}	—
High-pressure gas lasers (electron-beam-pumped)	4.8 – 8.5* (CO) 9.1 –11.3* (CO_2)	—	—

*Predicted.

2.1. Organic dye lasers

Tunable organic dye lasers are available commercially, covering the wavelength range from the near ultra-violet to slightly over 1 μm in the infra-red. They operate by optical pumping from the ground state to an excited singlet electronic state of high rotational and vibrational energy [7]. Subsequently the vibration-rotation energy is thermalized by very rapid non-radiative relaxation. A population inversion then exists, and stimulated emission occurs between low vibration-rotation energy levels of the first excited singlet electronic state and higher vibration-rotation levels of the ground electronic state (according to the Franck-Condon principle). Due to the high density of vibration-rotation levels of the large dye molecules and the large widths of these levels in solution, very broad, continuous bands of radiation are emitted (typically several hundred angstroms wide). Narrow-linewidth lasing, tunable within the broad emission band is achieved by the use of highly frequency-selective optical resonators.

Lasers have been made from dyes of the oxazole, xanthene, anthracene, coumarin, acridine, azine, pthalocyanine and polymethine families. Using various dyes, pulsed operation has been obtained from 0.34 to 1.2 μm, with both flash lamps and lasers (notably N_2 and ruby) used as pumps. Linewidths as narrow as 7 MHz have been obtained with an external Fabry-Perot [8]. Peak powers of 10^7 W, and average powers of the order of 1 W [8a] have been observed.

2.2. Optical parametric oscillators

Commercial versions of optical parametric oscillators surpass the dye laser in infra-red tunability, extending the available range to almost 4 μm. An optical para metric oscillator requires a laser pump source impinging onto a non-linear crystal. The resulting radiation can be tuned over a wide wavelength range by changing the temperature or orientation of the crystal [9].

A doubled Nd:YAG-laser-pumped oscillator using $LiNbO_3$ as the non-linear element can tune from 0.55 to 3.75 μm with a bandwidth of 1 cm^{-1} in the visible and less than 0.25 cm^{-1} in the infra-red; with single pulse energy of 1 mJ and repetition rates up to 1000 pulses per second. Using a ruby laser pump source, a spectral region from about 1 to 4 μm can be covered with pulse energies of approximately 0.1 J. The spectral width typically 0.25 cm^{-1} is determined by the crystal length, but it can be reduced by using an intracavity etalon. A bandwidth of 30 MHz (0.001 cm^{-1}) has been recently reported in the vicinity of 2.5 μm for a pulsed $LiNbO_3$ doubled Nd:YAG oscillator using a novel interferometer mode-selector scheme [10]. Recently, parametric oscillation in the 10 μm region has been achieved in the laboratory [11], indicating that this tunable source can potentially cover all of the important infra-red "fingerprint" region between 3 and 15 μm.

2.3. Semiconductor diode lasers

Semiconductor diode lasers can be tailored to emit in desired wavelength regions by control of the energy gap a feature made possible by the development of ternary semiconductor compounds of adjustable chemical composition [12]. The different materials from which semiconductor lasers have been made are shown in Fig. 1. Complete coverage of the region between 0.63 and 34 μm is now possible. The dashed

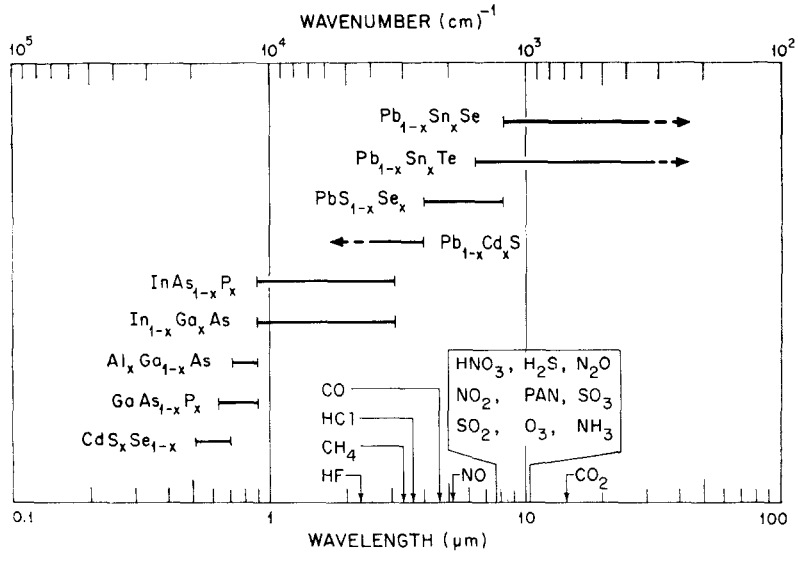

Figure 1 Wavelength ranges for semiconductor lasers made from different alloys and compositions. Also shown are some strongly-absorbing regions for several common atmospheric pollutants.

lines indicate possible future extension of the present limits (solid lines). Most of the tunable diode laser work has been performed with the lead chalcogenides $Pb_{1-x}Sn_xTe$ (between 6.5 and 34 μm), $PbS_{1-x}Se_x$ (between 4.0 and 8.5 μm), and $Pb_{1-x}Cd_xS$ (between about 2.5 and 4 μm). Principal absorbing wavelengths of some of the important pollutant gases are indicated at the bottom of this figure. It should be noted that with these three semiconducting compounds, nearly all of the important pollutants can be detected.

Fig. 2 shows a semiconductor diode laser in its standard package, which is 1 cm in overall length. (The entire unit is approximately the size of an average transistor.) The

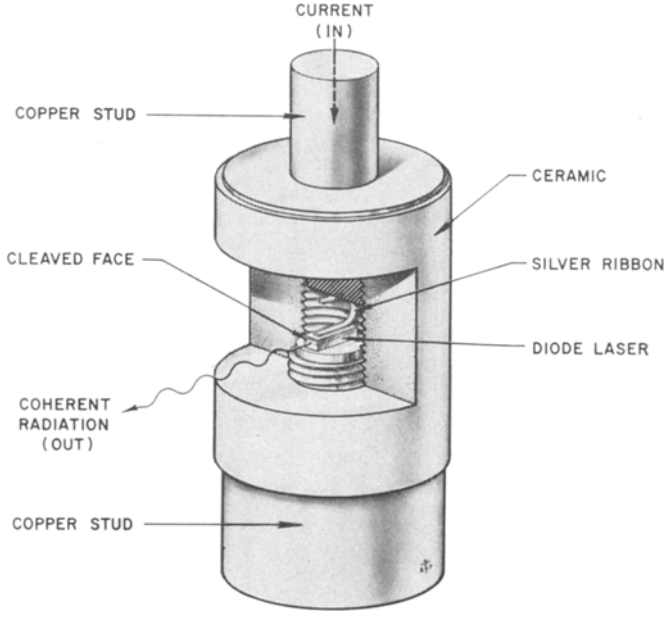

Figure 2 Semiconductor diode laser in a standard package having an overall length of 1 cm. The laser itself has approximate dimensions of 0.12 × 0.05 × 0.03 cm. Tuning is accomplished by changing the direct current applied to the diode.

diode crystal is mounted on a copper stud, which serves as one electrical contact. A silver ribbon serves as the other contact. Laser emission is produced by passing a current through the diode; this current can be supplied by a small battery or d.c. power supply for CW operation, or by a pulser for pulsed operation. There are several ways to "tune" a diode laser, the simplest being to change the magnitude of an applied direct bias current, which changes the junction temperature through heating [13]. Since the refractive index within the laser cavity is temperature-dependent, the laser wavelength changes. Although this type of tuning is thermal, it is still relatively fast because of the limited volume involved. Modulation frequencies of several hundred Hertz can be applied before thermal inertia becomes very noticeable; and useful experiments have been carried out with frequencies as high as 10 kHz.

Current-tuned semiconductor diode lasers have been used to perform Doppler-limited spectroscopy on several gases: SF_6, NH_3, C_2H_4 in the 10 μm region [14, 2], NO, CO, and water vapour around 5 μm [15], and an extensive study of the ν_1 band of SO_2 in the 8.7 μm region [16].

At present, the greatest obstacle to broader application of semiconductor lasers is their requirement for cryogenic cooling. Large improvements in efficiency are expected to relax these cooling requirements to the point where pulsed operation even at wavelengths as long as 10 μm will be possible at temperatures above 100 K.

2.4. Spin-flip Raman laser

The spin-flip Raman laser is a device which uses a fixed-frequency laser (at present, a CO or CO_2 gas laser) to pump a semiconductor crystal at cryogenic temperatures and in a magnetic field [17]. The pump laser photons lose energy when they collide with electrons in the crystal and flip their spin. The down-shifted Raman photon is separated in energy from the pump photon by the magnitude of the electron spin energy $g\beta H$, where g is the conduction electron g-factor, β the Bohr magneton, and H the magnetic field strength. Consequently, the output frequency depends on the magnetic field.

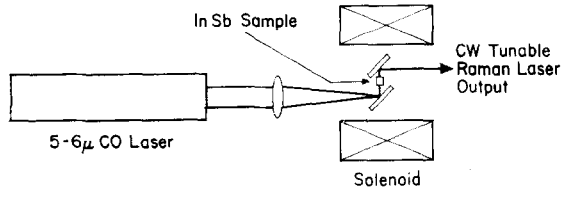

Figure 3 Experimental arrangement for a CW spin-flip Raman laser consisting of an InSb semiconductor crystal pumped with a CO gas laser. The magnetic field produced by the solenoid controls the electronic energy levels within the semiconductor, permitting wavelength-tuning.

A schematic drawing of a spin-flip Raman laser using a CO laser pump and InSb semiconductor is shown in Fig. 3. A linewidth of 1 kHz for the tunable laser radiation has recently been reported by Patel on the basis of heterodyne measurements [18]. The spin-flip Raman laser has been used to obtain spectroscopic data of NH_3 in the 10 μm region [19] and of NO around 5 μm [20].

2.5. Optically-pumped semiconductor lasers

A Q-switched Nd:YAG laser has been used to pump samples of the ternary compound semiconductor $In_xGa_{1-x}As$ at room temperature, producing laser radiation at 1.09 and 1.12 μm [21]. Recently, Melngailis achieved CW laser emission from a liquid-helium-cooled $Pb_{0.88}Sn_{0.12}Te$ crystal pumped with a GaAs diode laser [21a]. It appears that, by using commercially-available GaAs diode lasers as pump sources, tunable semiconductor lasers can be made which have some of the advantages of gas lasers, such as high output power and good beam quality, in addition to the relative simplicity, ruggedness, and small size characteristic of diode lasers.

2.6. High-pressure gas laser

At pressures of 10 to 15 atmospheres, adjacent vibration-rotation lines, which are responsible for emission in gas lasers, overlap such that lasing can occur at intermediate wavelengths as well. At present, electron-beam excitation is required for this potentially powerful tunable source of infra-red radiation, and several laboratories are investigating its potential for spectroscopic applications [22].

3. Monitoring techniques

Comparison is often made between tunable laser techniques and those involving conventional infra-red instrumentation for air pollution monitoring. The laser system usually has better sensitivity and specificity because of its higher usable power in a narrow spectral bandwidth, compared with that available from thermal sources. A comparison of resolution is illustrated in Fig. 4, where a diode laser beam at 10 μm was transmitted through a laboratory-quality grating spectrometer with narrow (80 μm

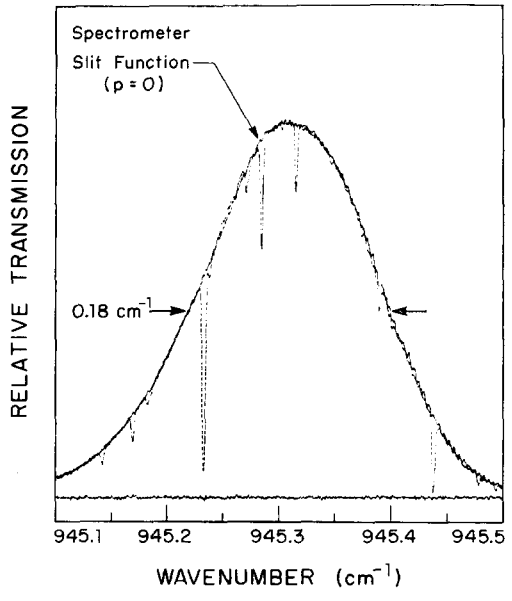

Figure 4 Transmission of tunable $Pb_{0.88}Sn_{0.12}Te$ diode laser radiation through a grating spectrometer with 80 μm slits, showing the bell-shaped slit function. The narrow absorption lines are produced when 0.5 torr of C_2H_4 was introduced into a 30 cm long cell in front of the spectrometer.

wide) slits. The smooth bell-shaped curve represents the spectrometer slit function, with a half-width (resolution) of 0.18 cm^{-1}. The narrow absorption lines were produced by introducing 0.5 torr of ethylene into a 30 cm long gas cell in front of the spectrometer. These lines are predominantly Doppler-broadened to a width of 66 MHz (0.0022 cm^{-1}). The laser linewidth itself is two or three orders of magnitude narrower than this [23]. It is clear that any attempt to use this spectrometer to evaluate the high-resolution spectra of ethylene will suffer, both in terms of sensitivity and specificity, because of

overlap and a severe reduction in intensity produced by the relatively wide spectral interval accepted by the instrument.

For actual *in situ* measurements, spectral lines of pollutant gases which are this narrow would only occur at very high altitudes, in and above the stratosphere. Nevertheless, even at ground level where atmospheric pressure broadens these ethylene lines to a value of approximately 0.2 cm^{-1}, some instrumental broadening will be produced by even this spectrometer; and substantially more by one which can be used in the field.

Three fundamental monitoring techniques employing tunable lasers are: remote heterodyne detection, resonance fluorescence, and direct absorption. Each has its particular advantages and applications, as described below.

3.1. Remote heterodyne detection

This technique represents a completely passive, single-ended laser system for the detection of gaseous pollutants from stationary or mobile sources. Characteristic infra-red emission lines from a pollutant gas are detected by heterodyning them with tunable laser radiation of the same wavelength, using the configuration of Fig. 5. The laser

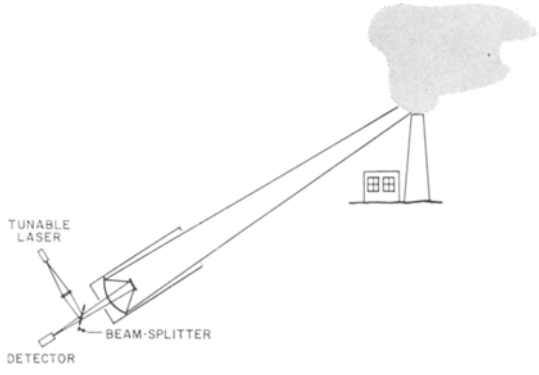

Figure 5 Configuration for remote heterodyne detection of pollutant gases from a smokestack using a tunable-diode-laser local oscillator.

radiation and that from the source are directed onto a wide-band infra-red detector cooled to liquid helium temperatures. By scanning the laser wavelength through that of the pollutant emission line, a beat frequency is produced whenever the difference frequency between the two infra-red signals is within the bandpass of the detector/amplifier system; the amplitude of the signal is related to pollutant concentration. The signal-to-noise ratio is given by [2]

$$\frac{S}{N} = [1 - \exp(-\alpha'_c cL)] \left[\frac{1}{\exp(h\nu/kT_g) - 1} - \frac{\epsilon_b}{\exp(h\nu/kT_b) - 1}\right] [B\tau]^{1/2}, \quad (1)$$

where α'_c is the absorption coefficient of the line per ppm of gas concentration (c), L the thickness of the plume, T_g its temperature, ϵ_b the emissivity of the background at

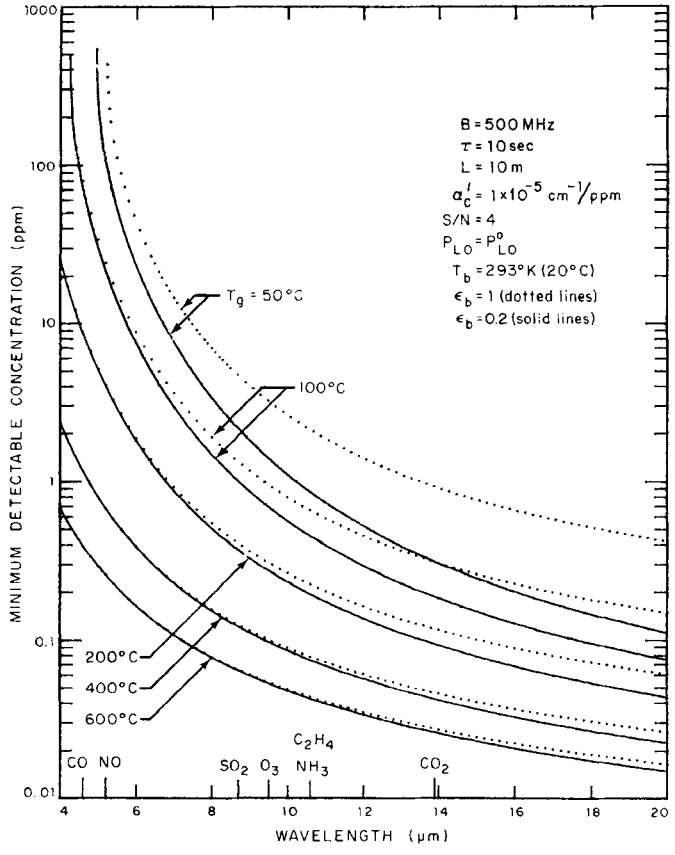

Figure 6 Theoretical wavelength dependence for remote heterodyne pollutant monitoring for various gas temperatures, and for background emissivities of 0.2 and 1.0. Useful wavelengths for some pollutant gases are indicated on the abcissa. Other parameters are shown in the figure.

temperature T_b, ν is the infra-red frequency, h is Planck's constant, k is Boltzmann's constant, B the system bandwidth and τ the post-detection integration time. Equation 1 is also based on the following assumptions: (i) that the IF bandwidth is less than the emission linewidth; (ii) that the emission and absorption due to the pollutant in the ambient atmosphere is not important because of a low concentration there relative to that in the plume; (iii) that the background attenuation from the wings of other molecular absorption lines is negligible; and (iv) that the local oscillator has sufficient power to overcome the other sources of noise. Equation 1 holds, regardless of range, as long as the field of view of the collecting telescope is fully subtended by the plume; in the infra-red, with collection optics only a few centimetres in diameter, it should be possible to detect pollutants 1 kilometre away.

Under these conditions the minimum detectable concentrations for pollutant gases with line strengths of 1×10^{-5} cm^{-1}/ppm are shown in Fig. 6 as a function of wavelength and for different source temperatures and background emissivities. Concentrations of a few ppm of NO and CO at 400 to 600° C can be detected; and similar sensitivities are

achievable for C_2H_4 and NH_3 (at longer wavelengths) at a temperature of only 50° C. Since SO_2 in the 8.7 μm region has a measured absorption strength almost ten times smaller, the minimum detectable concentrations for this gas should be raised accordingly.

The local oscillator power necessary to satisfy assumption (iv) above is given by the equation [24]

$$P_{LO}^{\circ} = \frac{(kT_A)\,(h\nu)}{\eta e^2 G^2 R_L}\,, \tag{2}$$

where T_A is the noise temperature of the amplifier, G the infra-red detector gain and η its quantum efficiency, R_L the load resistance, and e the electronic charge. For an amplifier with a noise temperature of 240 K (noise figure of 2.4 dB), and assuming $\eta = 0.5$, $G = 0.12$, $R_L = 50$ ohms, and $\lambda = c/\nu = 10$ μm, we obtain $P_{LO}^{\circ} = 12$ mW.

Using state-of-the-art infra-red detectors and low-noise amplifiers, the local oscillator power of 12 mW is prohibitive, producing not only excessive heating of the detector, but a substantial liquid helium boiloff. When wideband ($\gtrsim$ 500 MHz) photodiodes having nearly unit quantum efficiency become available, the local oscillator power requirement will be less than 100 μW, a more realistic value. Experimentally, heterodyne theory has been confirmed by measurements of thermal radiation from a calibrated source; and lines from hot ethylene (600 K) near 10 μm were detected using a CO_2 laser as local oscillator and a Ge:Cu photoconductor as infra-red detector [3].

3.2. Resonance fluorescence

Absorption of tunable laser light, and detection of subsequent re-radiation, can be used for remote single-ended detection. Because the laser radiation is directed into the atmosphere, this technique is active, rather than passive. Fluorescence can be excited by pumping either at vibrational frequencies of the molecules, which require lasers at infra-red wavelengths, or at electronic transition frequencies, which fall in the visible or ultra-violet part of the spectrum. Several gases, such as SO_2, O_3, NO, NO_2, NH_3, HCOH (formaldehyde) and C_6H_6 (benzene) have absorption bands in the ultra-violet. However, there is a potential problem due to overlap between individual bands, some of which are quite broad. Moreover, atmospheric transparency becomes poor as we approach the vacuum ultra-violet. The electronic transitions should be important for detecting metal vapours such as As, Be, Cu, Zn, Na, and Hg. Atomic sodium has been detected at altitudes of about 90 km, in concentrations of the order of $10^4/cm^3$ using a dye laser tuned to the D lines [25]. For resonance fluorescence in the infra-red, Kildal and Byer [4] predict that with a tunable optical parametric oscillator at 4.7 μm, emitting 1 mJ pulses, 100 ns wide, with a 0.1 cm^{-1} spectral width, it should be possible to detect 2 ppm of CO at a range of 100 m.

3.3. Absorption

Direct absorption of tunable laser radiation offers the greatest versatility of the three schemes discussed. Point sampling at reduced pressure permits very high specificity as the infra-red "signatures" of pollutant gases become observable. Accordingly, this

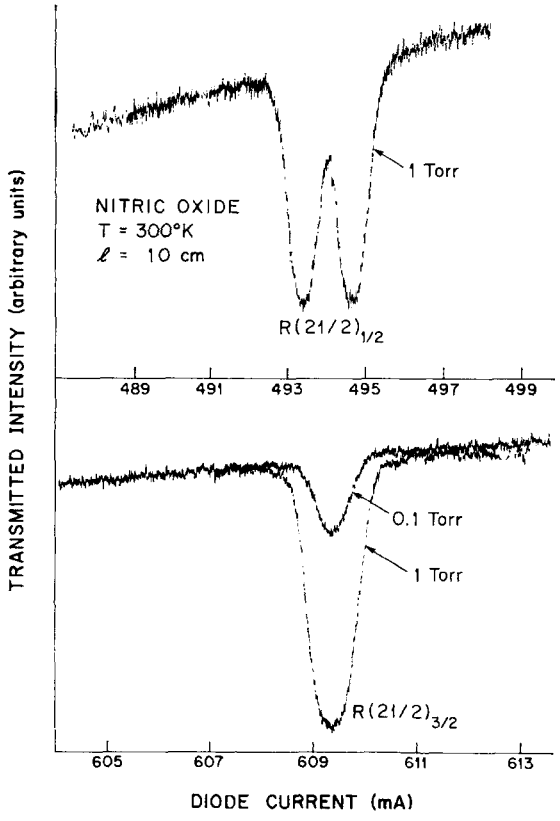

Figure 7 Tunable $PbS_{0.60}Se_{0.40}$ diode laser scans of two NO lines in the 1912.1 cm^{-1} region. Lambda-doubling of the $R(21/2)_{1/2}$ line is 300 MHz wide (0.01 cm^{-1}). After Nill, *et al* [15].

technique can also be used to calibrate other instrumentation used for point-sampling. *In situ* source monitoring can be performed by transmitting the laser radiation across the effluent stream, leaving the stream itself essentially undisturbed. Transmission of tunable laser radiation over long atmospheric paths can be used to attain the high sensitivity required for ambient-air monitoring.

3.3.1. Point sampling

In point-sampling applications the total gas pressure can be lowered to reduce or eliminate completely any overlap between adjacent vibration-rotation lines; consequently, very high specificity is possible. One example of this is shown in Fig. 7, containing tunable $PbS_{0.60}Se_{0.40}$ diode laser scans of NO in the 5.2 μm region [15]. The characteristic Lambda-doubling of the $R(21/2)_{1/2}$ line at 1912.1 cm^{-1} in the upper trace is an unmistakable "signature" for this gas. Recently, Brueck, Johnson, and Mooradian have observed Lambda-doubling of the $R(1/2)_{1/2}$ line of NO at 1881.0 cm^{-1} using a CO-pumped spin-flip Raman laser [20].

Kreuzer and Patel [20] have used a 50 mW spin-flip Raman laser in conjunction with an opto-acoustic cell (spectrophone) to detect NO in both the ambient air and in

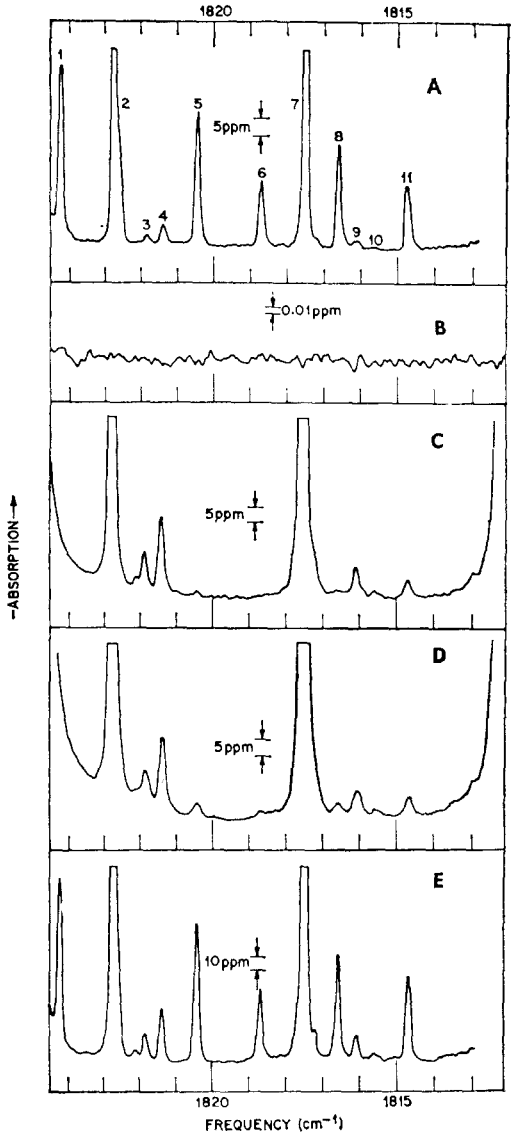

Figure 8 Detection of NO with an opto-acoustic detector using a tunable spin-flip Raman laser: (A) calibration scan of 20 ppm NO in N_2; (B) noise level with laser blocked; (C), (D), and (E) are scans for samples of laboratory atmosphere, ambient air near a busy highway, and exhaust gas from an automobile, respectively. All measurements were performed at approximately 300 torr total pressure. Lines 1, 5, 6, 8, and 11 are due to NO, the rest are caused by water vapour. Reprinted with permission of the American Association for the Advancement of Science. After Kreuzer and Patel [20].

samples of automobile exhaust. By using a mechanical chopper to modulate the intensity of the laser beam, acoustic pulses produced in the cell when the laser is tuned to an absorption line can be detected with a capacitive microphone, analogous to the operation of a Golay cell. Some of their measurements are shown in Fig. 8. Trace A

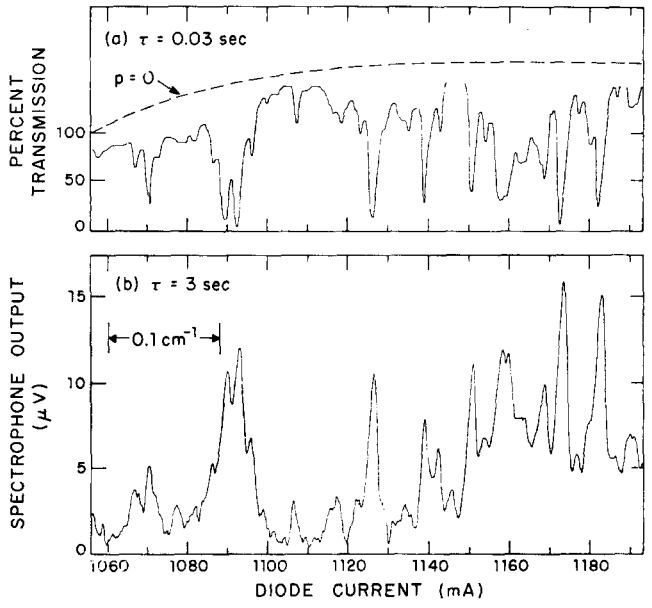

Figure 9 (a) Transmission scan for C_2H_4 in air using a $Pb_{0.88}Sn_{0.12}Te$ diode laser in the 10 μm region and a liquid-helium-cooled Ge:Cu detector. (b) Absorption scan over the same spectral region using opto-acoustic (spectrophone) detection. Cell length is 10 cm, C_2H_4 pressure is 5 torr, and the air pressure is 15 torr.

is a calibration scan of 20 ppm NO in N_2 at a total pressure of 300 torr. The lines designated as 1, 5, 6, 8, and 11 are due to NO, while the others represent water vapour. Trace B shows the noise level with the laser radiation blocked, which is primarily Johnson noise in the first amplifier stage [26]. The concentration of NO in a sample of ambient air is estimated to be approximately 0.1 ppm on the basis of Trace C. A sample from a busy road, Trace D, shows a somewhat higher NO content of 2 ppm. In Trace E the amount of NO in an exhaust specimen from an automobile is seen to be over 50 ppm.

The spectrophone is useful for detecting absorbed tunable laser radiation because it is sensitive (for tunable lasers with moderate power levels), independent of wavelength, and operates at room temperature. An experiment was performed to compare the *absorption* signal from a spectrophone with the simultaneously *transmitted* signal through the cell, monitored with a liquid-helium-cooled Ge:Cu infra-red detector. A tunable $Pb_{0.88}Sn_{0.12}Te$ diode laser was used, and the radiation was chopped mechanically before entering the cell. The lower trace of Fig. 9 is the spectrophone signal proportional to the absorbed laser power p_a; the upper trace represents the infra-red detector signal, proportional to transmitted power p_t, where the dashed line corresponds to 100% transmission. The traces are seen to resemble the expected relation to each other, according to the expression $p_t = 1 - p_a$.

By frequency-modulating the laser emission, rather than using amplitude-modulation the signals for transmission and absorption should be identical, except for phase.

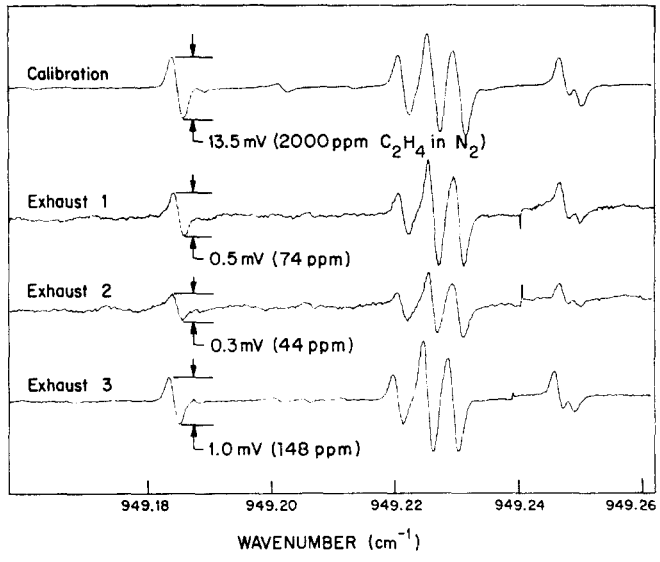

Figure 10 First-derivative spectra, taken with a $Pb_{0.88}Sn_{0.12}Te$ diode laser, of: (a) a calibration sample of 2000 ppm C_2H_4 in N_2 (top trace), and three automobile exhaust samples at different amplifier gain settings. Total pressure, 5 torr; cell length, 30 cm.

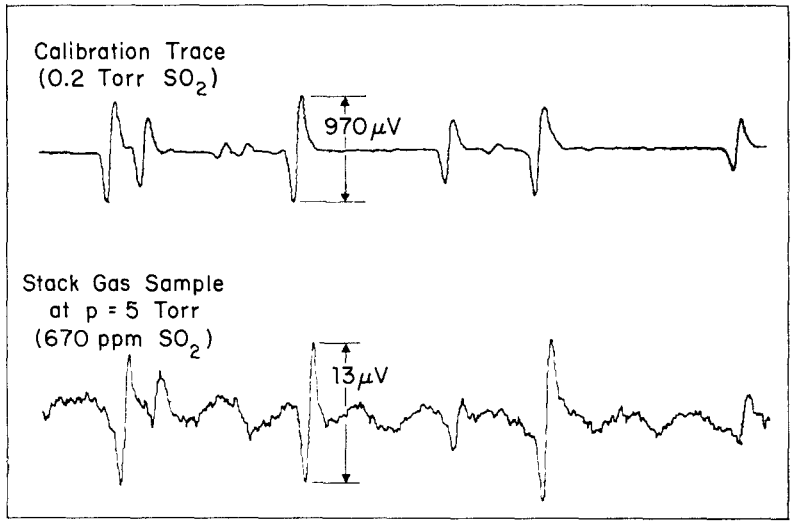

Figure 11 First-derivative spectra, taken with a $Pb_{0.93}Sn_{0.07}Te$ diode laser, of 0.2 torr SO_2 in the 8.7 μm region (upper trace), and a sample of stack gas reduced to 5 torr pressure (lower trace). Cell length, 730 cm.

Derivative detection was used to compare the minimum detectable concentrations of the two techniques. Using a 10 μm $Pb_{0.88}Sn_{0.12}Te$ diode laser having a CW power level of 6 μW, and a 10 cm long cell, the detection limit for C_2H_4 using the spectrophone was a few hundred ppm, whereas that employing the liquid-helium-cooled infra-red detector was 1 ppm under the same conditions. The absorption coefficient for the C_2H_4

line was approximately 10^{-6} cm^{-1}/ppm, yielding a total absorbed power of $P_0\alpha' cL = 6 \times 10^{-11}$W, which is close to the noise-equivalent-power of the Ge:Cu infra-red detector. Conversely, the Johnson noise limit for the spectrophone imposed by the high-impedance circuitry, is approximately 10^{-8}W [26], making the spectrophone less appropriate for systems involving tunable laser sources of relatively low power.

Frequency modulation of the laser emission eliminates the need for a mechanical chopper. For a semiconductor diode laser, this is accomplished by superimposing a small ($\sim$1 mA) sinusoidal current upon the steady current, and detecting the first derivative at the modulation frequency, or the second derivative at the first harmonic.

Figs. 10 and 11 illustrate application of this technique to the point-sampling of automobile and smokestack effluents. In Fig. 10 is a set of first-derivative scans for C_2H_4 near the Q branch of the ν_7 vibration-rotation band at 10.6 μm. The upper trace represents a 2000 ppm mixture of C_2H_4 in N_2, at a total pressure of 5 torr, and is used for calibration. The three lower traces were obtained for different samples of raw automobile exhaust, for which the total pressure was also reduced to 5 torr. The presence of C_2H_4 is unmistakable because of the identical signatures; and by comparing their amplitudes with that of the calibrated sample, a quantitative determination can be made of the C_2H_4 content of each. There is no noticeable interference by any of the other components such as water vapour, CO, NO, and other hydrocarbons, which are also present in large quantities.

Fig. 11 shows results for a similar study of SO_2 in a sample of stack gas from an oil-fired power plant. Using a tunable $Pb_{0.93}Sn_{0.07}Te$ diode laser in the 8.7 μm region of the ν_1 band, the derivative scan yields a value of 670 ppm for the concentration of SO_2 in the specimen. As with the automobile exhaust measurements, there appear to be no interferences from other gaseous components which are present. There is, however, a periodic background fluctuation caused by Fabry-Perot-type feedback from

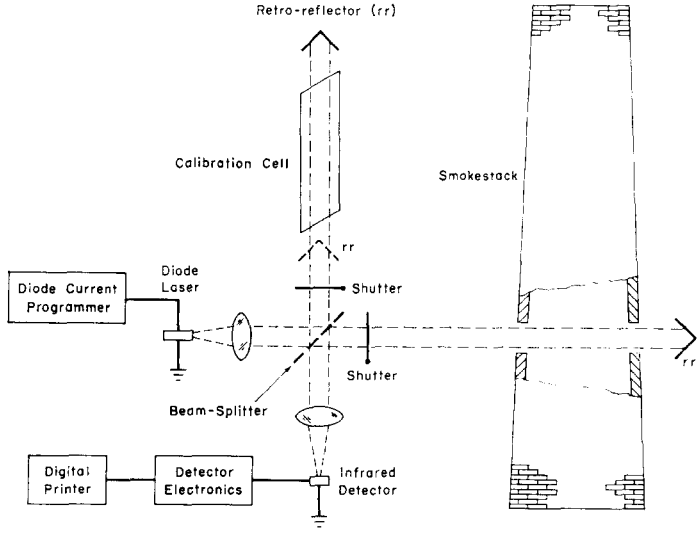

Figure 12 Diode laser system for across-the-stack monitoring of pollutant gases in a smokestack.

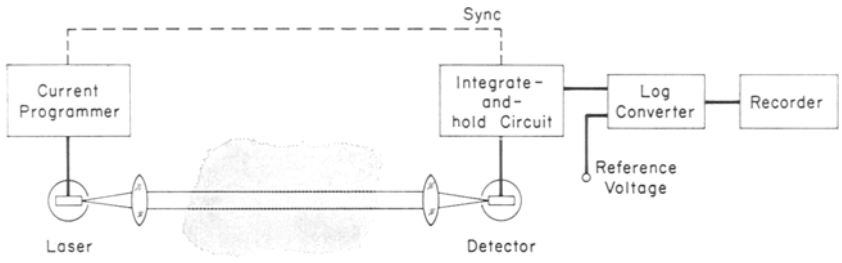

Figure 13 Operational schematic for general application of pulsed semiconductor diode lasers to the monitoring of atmospheric pollutants at emission sources or in the ambient air.

windows of the sample cell, which can be eliminated by proper design. It should be noted that these lines of SO_2 are not the strongest in the ν_1 band, and that the derivative signal would be twenty times larger if a more appropriate wavelength region were selected [16].

3.3.2. In situ *source monitoring*

A tunable-diode-laser system for across-the-stack monitoring of SO_2 is presently under construction at our laboratory. The system, which is illustrated in Fig. 12, yields an average value for the SO_2 concentration across the stack. This should be more representative than point-sampled values for predicting the total amount of SO_2 emitted into the environment. Preliminary work involved an extensive study of the 8.7 μm SO_2 band; the locations and strengths of over 200 lines were made by tunable diode laser spectroscopy, and compared with a theoretical model [16]. Other parameters, such as line-broadening coefficients, were also measured, and for SO_2 in the atmosphere the full linewidth at half-maximum intensity was found to be 0.3 cm^{-1}.

For the detection of pollutant gases in the atmosphere, where linewidths are relatively wide, pulsed-diode laser techniques can be used. By using pulses of current, rather than steady values, the cryogenic-cooling requirements are less stringent, and higher output laser powers can be achieved since larger injection currents are possible. The diode laser can still be tuned by a superimposed direct current. The power p_t received at the detector is related to the power p_0 from the laser by the Beer-Lambert equation

$$p_t = p_0 \exp\left[-\alpha'_c cL\right] , \tag{3}$$

where the other symbols were defined earlier. With the aid of an integrate-and-hold circuit in conjunction with a logarithmic detector, as shown in the schematic of Fig. 13, the recorded voltage is directly proportional to the pollutant concentration, c.

Application of this technique to on-line automobile exhaust monitoring was demonstrated by measurements made using a 1.15 m long optical path. Exhaust gas from an automobile was passed through a windowless tube through which the laser beam was also directed. Test results for a 1972 eight-cylinder station wagon are shown in Fig. 14* for two starting cycles: (a) a normal start where the accelerator pedal was not depressed; (b) a "rich" start. The measurement is essentially instantaneous, limited only by the rate of change of the C_2H_4 content in the exhaust. The C_2H_4 concentration of around

*The ordinate scale in Fig. 14 is incorrect. Instead of a maximum concentration of 1000 ppm, read 1500 ppm.

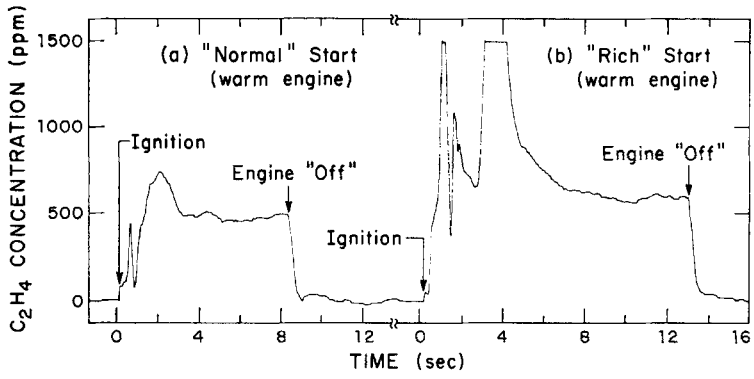

Figure 14 Results of an on-line emissions test for C_2H_4 in a 1972 station wagon, using a pulsed $Pb_{0.88}Sn_{0.12}Te$ diode laser operating at 10.57 μm. (a) represents a normal start of a warm engine, with ignition at time $t = 0$. For (b) the accelerator pedal was depressed during ignition, to produce a "rich" start, with significantly higher C_2H_4 emission.

300 ppm during idle was confirmed by taking a sample and using the first-derivative technique at reduced pressure, described earlier.

3.3.3. Ambient-air monitoring

For ambient-air monitoring, where pollutant levels are usually much lower than they are near sources, sensitive detection can be achieved by long-path transmission or with the aid of multi-reflection cells. Although multi-reflection cell techniques are very susceptible to mirror contamination, tunable lasers can, by scanning alternately "on" and "off" an absorption line, eliminate most of the adverse effects caused by such variations in reflectivity. Of course, consideration must be given to the atmospheric "windows" when selecting appropriate wavelength regions.

At low pollutant concentrations, Equation 3 can be approximated as follows:

$$p_t \simeq p_0(1 - \alpha'_c c_m L) \equiv p_0 - \delta_p \tag{4}$$

where δ_p is the minimum detectable change in power. Solving for the minimum detectable pollutant concentration c_m, we obtain

$$c_m = \frac{\delta_p}{p_0 \alpha'_c L} . \tag{5}$$

Under laboratory conditions, presently available infra-red detectors can detect power variations of less than 10^{-11} W. In actual application, however, fluctuations in received laser power imposed by atmospheric turbulence, scattering, and equipment vibration may degrade this value. If we assume that the minimum detectable power δ_p is 10^{-9} W, that the laser power p_0 is 100 μW, $\alpha'_c = 10^{-5}$ cm^{-1}/ppm, and a path length L of 500 m, the minimum detectable concentration c_m is 0.02 ppb.

We have recently transmitted 10.6 μm radiation from a $Pb_{0.88}Sn_{0.12}Te$ diode laser over a 500 m path, with a collection efficiency of 33%. The system used the electronic schematic shown in Fig. 13. With the beam directed horizontally about 4.5 m above a parking lot, an average increase of several ppm of C_2H_4 was detected during the late

afternoon exodus of automobiles. The noise level for this test, with 2 μW of received laser power, was 120 ppb, caused primarily by relative vibrations in the optics.

4. Conclusion

There appear to be several important uses of tunable lasers for the monitoring of atmospheric pollutants, and some systems are already under construction. This field is very new, less than two years old for the most part, and although requirements of low-temperature operation limit widespread use of some tunable lasers at present, improvements in both laser technology and advances in cryogenic cooler development should eventually eliminate this drawback for future monitoring applications.

Acknowledgements

The author would like to thank H. A. Pike for permission to use pre-publication results of his spectrophone measurements and on-line automobile emissions data, R. S. Sinclair for designing the electronic circuitry for pulsed-laser monitoring, A. R. Calawa and T. C. Harman for developing the diode lasers, and K. W. Nill and F. A. Blum for providing their nitric oxide spectra. Appreciation is also expressed to J. O. Sample, T. E. Stack, and L. B. McCullough for very competent technical assistance.

References

1. For a comprehensive review, including an extensive set of references to earlier work, see P. L. HANST, "Advances in Environmental Science and Technology", Volume 2, edited by James N. Pitts and Robert L. Metcalf (John Wiley, New York, 1971) chapter 4.
2. E. D. HINKLEY and P. L. KELLEY, *Science* **171** (1971) 635-639.
3. E. D. HINKLEY and R. H. KINGSTON, Proceedings of the Joint Conference on Sensing of Environmental Pollutants, Palo Alto, California, 8-10 November, 1971.
4. H. KILDAL and R. L. BYER, *Proc. IEEE* **59** (1971) 1644-1663.
5. I. MELNGAILIS, *IEEE Trans. on Geoscience Electronics* **GE-10** (1972) 7-17.
6. C. F. DEWEY, JUN., and L. O. HOCKER, *Appl. Phys. Lett.* **18** (1971) 58-60.
7. D. J. BRADLEY, Proc. Electro-Optical Systems Conference, Brighton, England, March, 1971; B. B. SNAVELY, *Proc. IEEE* **57** (1969) 1374-1390.
8. T. W. HANSCH, I. S. SHAHIN, and A. L. SCHAWLOW, *Phys. Rev. Lett.* **27** (1971) 707-710.

8a. S. S. TUCCIO and F. C. STROME, JUN., *Appl. Optics* **11** (1972) 64-73; A. DIENES, E. P. IPPEN, and C. V. SHANK, *IEEE J. Quantum Electron.* **8** (1972) 388.

9. S. E. HARRIS, *Proc. IEEE* **57** (1969) 2096-2113; R. G. SMITH, Optical Parametric Oscillators, in "Laser Handbook", edited by F. T. Arrechi and E. O. Schultz-DuBois (North-Holland Publishing Company, Amsterdam) (to be published).
10. J. PINARD and J. F. YOUNG, *Optics Comm.* **4** (1972) 425-427.
11. R. L. BYER, VII International Quantum Electronics Conference, Montreal, Canada, 8-11 May, 1972.
12. For a general review, with extensive references, see T. C. HARMAN, "The Physics of Semimetals and Narrow-Gap Semiconductors", edited by D. L. Carter and R. T. Bate, proceedings of the Conference held in Dallas, Texas, 1970 (Pergamon Press, New York); also T. C. HARMAN, *J. Phys. Chem. Solids Supplement* **32** (1971) 363-382.
13. E. D. HINKLEY, T. C. HARMAN, and C. FREED, *Appl. Phys. Lett.* **13** (1968) 49-51.
14. E. D. HINKLEY, *ibid* **16** (1970) 351-354.
15. K. W. NILL, F. A. BLUM, A. R. CALAWA, and T. C. HARMAN, *ibid* **19** (1971) 79-82; *Chem. Phys. Lett.* (to be published).

16. E. D. HINKLEY, A. R. CALAWA, P. L. KELLEY, and S. A. CLOUGH, *J. Appl. Phys.*, July, 1972 (to be published).
17. C. K. N. PATEL and E. D. SHAW, *Phys. Rev. Lett.* **24** (1970) 383-385; A. MOORADIAN, S. R. J. BRUECK, and F. A. BLUM, *Appl. Phys. Lett.* **17** (1970) 481-483.
18. C. K. N. PATEL, *Phys. Rev. Lett.* **28** (1972) 649-652.
19. C. K. N. PATEL, E. D. SHAW, and R. J. KERL, *ibid* **25** (1970) 8-11.
20. L. B. KREUZER and C. K. N. PATEL, *Science* **173** (1971) 45-47; R. A. WOOD, R. B. DENNIS, and J. W. SMITH, *Optics Comm.* **4** (1972) 383-387; S. R. J. BRUECK, E. J. JOHNSON, and A. MOORADIAN (private communication).
21. J. A. ROSSI, S. R. CHINN, and A. MOORADIAN, *Appl. Phys. Lett.* **20** (1972) 84-86.
21a. I. MELNGAILIS (private communication).
22. V. N. BAGRATASHVILI, I. N. KNYAZEV, and V. S. LETOKHOV, *Optics Comm.* **4** (1971) 154-156; N. G. BASOV, E. M. BELENOV, V. A. DANILYCHEV, and A. F. SUCHOV, *Quantum Electron. (USSR) N*3 (1971) 121-122; C. A. FENSTERMACHER, M. J. NUTTER, W. T. LELAND, and K. BOYER, *Appl. Phys. Lett.* **20** (1972) 56-60.
23. E. D. HINKLEY and C. FREED, *Phys. Rev. Lett.* **23** (1969) 277-280.
24. R. J. KEYES and T. M. QUIST, "Semiconductors and Semimetals", edited by R. K. Willardson and A. C. Beer (Academic Press, New York, 1970), chapter 8.
25. M. R. BOWMAN, A. J. GIBSON, and M. C. W. SANDFORD, *Nature* **21** (1969) 456-457.
26. L. B. KREUZER (private communication).